energies

Article

Modeling and Simulation Analysis of Photovoltaic Photothermal Modules in Solar Heat Pump Systems

Tianbao Sun [1], Zhun Li [1,*], Yujun Gou [2,*], Guangzheng Guo [2], Yue An [2], Yongqi Fu [2], Qingan Li [3] and Xiaohui Zhong [3]

[1] China Institute of Metrology, Beijing 100029, China; suntb@nim.ac.cn
[2] College of Metallurgy and Energy, North China University of Technology, Tangshan 063210, China; guoguangzheng9708@163.com (G.G.); ay2059916@163.com (Y.A.); fyq225523@163.com (Y.F.)
[3] Institute of Engineering Thermophysics, Chinese Academy of Sciences, Beijing 100190, China; liqingan@iet.cn (Q.L.); zhongxiaohui@iet.cn (X.Z.)
* Correspondence: lizhun@nim.ac.cn (Z.L.); hbtsgyj2008@163.com (Y.G.)

Abstract: A solar heat pump based on the photovoltaic photothermal (PV/T) module is a new technology that can improve the photovoltaic efficiency and recovery of waste heat in photovoltaic conversion. The comprehensive efficiency of a system can thus be greatly improved. At present, there is little research on the simulation of a solar heat pump based on the Simulink 2018 software. In this paper, PV/T modules are modeled and simulated using the Simulink software based on the typical meteorological parameters in Beijing city during summer and winter conditions. Considering the system characteristics of a simultaneous operation, the models of all components such as the compressor, condenser, evaporator, expansion valve, and heat storage tanks contained in a system are established based on the system's working principle, energy conservation equations, and some empirical formulas and then simulated. As PV/T modules are the key influencing factor for system performance, the model and simulation process are introduced in detail in this paper. The results show that the surface temperature of PV/T modules under different operating conditions are all significantly lower than that of ordinary photovoltaic panels. The average temperature of PV/T modules is only 15.2 °C, which is 20.2 °C lower than that of ordinary panels under summer conditions, and the average temperature of PV/T modules is only 0.5 °C, 17.8 °C lower than that of ordinary panels under winter conditions. The average photoelectric efficiency can be improved by 15.4% and 8.9%. And, the temperature change amplitude of PV/T modules is lower, which weakens the temperature fluctuation of the modules. The photovoltaic efficiency is therefore further increased. As a result, the power generation and photovoltaic efficiency are both improved significantly.

Keywords: PV/T modules; solar heat pump; systems; Simulink

Citation: Sun, T.; Li, Z.; Gou, Y.; Guo, G.; An, Y.; Fu, Y.; Li, Q.; Zhong, X. Modeling and Simulation Analysis of Photovoltaic Photothermal Modules in Solar Heat Pump Systems. *Energies* **2024**, *17*, 1042. https://doi.org/10.3390/en17051042

Academic Editor: Ioan Sarbu

Received: 4 January 2024
Revised: 16 February 2024
Accepted: 19 February 2024
Published: 22 February 2024

1. Introduction

Recently, PV/T modules have become the key component in solar heat pump system development [1]. PV/T modules can achieve a combination of photoelectric and photothermal conversions, effectively reducing the surface temperature of photovoltaic modules and improving the photovoltaic conversion efficiency as the remaining heat is transferred. Furthermore, PV/T modules can collect the remaining heat as a low-temperature heat source for their connected heat pumps [2]. Scholars have conducted much research on PV/T heat pump systems. Kern [3] proposed the concept of a PV/T (photovoltaic thermal) solar energy system in which heat collection equipment is installed on the back of cells to recover heat. Ito [4] conducted experimental research on photovoltaic modules used as the evaporator of a heat pump and found that the system performance coefficient increased with increasing irradiance. Gang [5] studied a solar heat pump system with PV/T modules installed, and the results showed that the COP of the heat pump could reach up to 6.3 and that the performance coefficient even reached up to 9.0. Ji [6] and Zhang [7] proposed that the solar photovoltaic thermal heat pump system is a combination of a PV/T module and a heat pump. Solanki [8] developed a thermal model based on the energy balance equations. Shyam [9] studied a series combination of N PVT water collectors with different configurations covered with photovoltaic modules. Jouhara [10] designed a novel flat heat pipe-based thermal and PV/T (photovoltaic and thermal system) solar collector that can be used as an energy-active building envelope material. Li Hong [11] studied a new type of solar photovoltaic loop heat pipe/heat pump and analyzed the system performance under various operating modes. Chen [12] constructed a PV/T heat pump system with a micro heat pipe array and analyzed the increasing thermoelectric efficiency of the system. Chu [13] proposed a photovoltaic direct-driven PV/T dual-source heat pump system with hot water and studied the performance of the system.

With the improvement in computer computing power, numerical simulation technology has also been applied to research on PV/T solar heat pump systems [14]. Mastrullo [15] studied the model of a heat pump whose evaporator operates as a photovoltaic collector, and the energy balance equations were used for some heat pump components. Khelifa [16] used ANSYS to conduct a thermodynamic analysis of the PV/T modules, and the results showed that the temperature of photovoltaic modules decreased by 15% to 20%. Chen [17] established a three-dimensional physical model of flat plate PV/T modules in CFD 2018 software and studied the effects of different pipe heights, flow rates, inlet temperatures, wind speed, and ambient temperatures on PV/T module performance. Zhou [18] investigated the effects of different tube arrangements on the performance of a system with a tube flat PV/T module through a numerical simulation. Kavian [19] used TRNSYS to construct photovoltaic ground source heat pump hybrid systems in different scenarios, using the optimization tool developed by MATLAB software (R2021a), and data exchange between TRNSYS and MATLAB was achieved. Dannemand [20] studied the performance of a new system consisting of a heat pump, a PV/T collector, and two heat storage tanks and established a simulation model of the system in the transient simulation software TRNSYS (version 18.0) to provide domestic hot water for buildings. Yerdesh [21] developed a numerical simulation model for predicting the performance of a solar collector and two-stage cascade heat pump combined water heating systems under Kazakhstan climatic conditions. Hamid [22] studied PV/T collectors with four different channel configurations, established numerical models, and evaluated their energy and thermal efficiencies. Heinz [23] used TRNSYS to simulate heat pumps, photovoltaics, and heat storage tanks combined with intelligent control systems to reduce the proportion of grid power supply. Ma [24] designed a PV/T heat pump system with four operating modes, established a system model using TRNSYS software, and analyzed the annual operation of typical rural residences.

At present, there are mainly two types of modeling and simulation research for heat pump systems, dynamic and quasi-steady-state, to obtain the transient response and dynamic operating rules [25–27]. In the current research, many researchers have conducted simulations for PV/T solar heat pump systems based on the TRNSYS software, while the modeling and simulation research based on Simulink software is still in its initial stages.

In this article, an entire solar heat pump system is modeled and simulated based on the Simulink software. The Simulink software is a visual simulation tool that has the advantages of strong applicability; a clear simulation structure and operation process; being close to reality; and high efficiency and flexibility, which is very suitable for the simulation of dynamic and embedded systems. The Simulink software also supports continuous sampling, discrete time sampling, and mixed sampling time modeling. The performance and efficiency obtained by a Simulink simulation have great significance for the construction of actual solar heat pump systems. The Simulation results provide insight into the operating characteristics of the system and determine the matching correlation of each equipment. The PV/T modules not only affect the photovoltaic efficiency but also affect the starting temperature of the evaporator connected with the modules, which will determine the performance of the entire solar heat pump system. So, the modeling process of PV/T modules is the main focus of this article, and the simulated operating characteristics are analyzed in detail.

2. Establishment of Mathematical Model for PV/T Modules

The principle of a solar heat pump system is shown in Figure 1. A system includes two circulations: the left medium circulation in the PV/T modules and the right refrigerant circulation in the heat pump. In the left circulation, the current generated by the photovoltaic is transmitted to the user through an inverter, and simultaneously, the medium absorbs the waste heat from the PV/T modules, driven by a pump, and enters the evaporator to release heat. In the right circulation, the refrigerant absorbs the heat in the evaporator. And then, the refrigerant is heated and pressurized to a relatively high temperature and pressure state by the compressor. Finally, the refrigerant enters the condenser and the heat is transferred to the heat storage tank connected to the condenser. During operation, all components within the system work simultaneously. The characteristics of each component will affect the operational performance of the whole system. Therefore, it is necessary to consider the coupling impact among different parts. All components contained in the heat pump system have been modeled, including the compressor, condenser, evaporator, expansion valve, heat storage tanks, and solar radiation. As analyzed above, a key factor that affects the system thermal performance is the temperature of the PV/T modules. This article focuses on the modeling process of the PV/T modules.

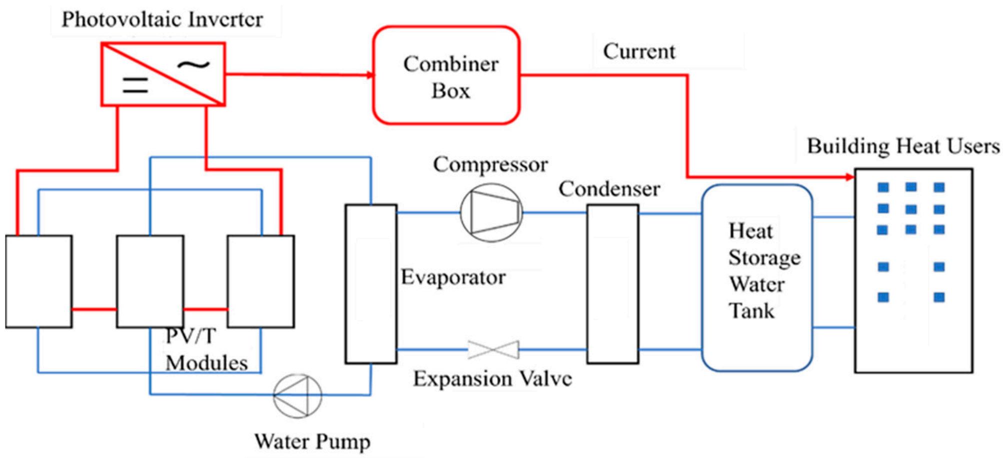

Figure 1. Schematic diagram of solar heat pump system.

2.1. Mathematical Modeling of PV/T Module

The structure of one PV/T module is shown in Figure 2a and consists of a glass cover plate, EVA adhesive, a photovoltaic panel, more EVA adhesive, a collector channel, and a insulation back plate from top to bottom. EVA is copolymerized from ethylene and acetic acid, which is widely used as a photovoltaic material. It plays multiple roles in bonding the inside of a PV/T photovoltaic thermal module, fixing the internal structure of the collector, and insulating to protect the photovoltaic panel.

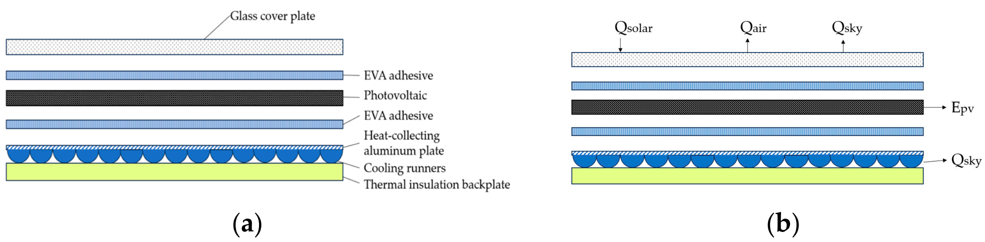

Figure 2. (**a**) Structural diagram of PV/T photovoltaic photothermal module; (**b**) energy conservation diagram of PV/T photothermal module.

The purpose of the simulation is to obtain the energy transfer process inside the PV/T photovoltaic thermal module. Therefore, the following assumptions are made to simplify the model and to reduce its computational complexity:

1. The temperature of each layer of the PV/T photovoltaic thermal module is uniform, and there is no temperature gradient within the same horizontal layer;
2. The heat transfer process only occurs in the direction perpendicular to the PV/T module;
3. The contact between different layers inside the module is good, without thermal conductivity or contact resistance;
4. The absorption and transmittance of the EVA adhesive to solar radiation is negligible;
5. The thermal properties of each layer of material are stable and do not change with temperature;
6. The insulation material has good insulation performance, without heat dissipation from the frame and back panel.

The energy conservation of the PV/T photovoltaic thermal module is shown in Figure 2b.

For the entire PV/T photovoltaic thermal module, its energy conservation equation can be written as follows [28]:

$$Q_{\text{solar}} = E_{\text{PV}} + Q_{\text{f}} + \rho_{\text{PV/T}} c_{\text{PV/T}} \delta_{\text{PV/T}} \frac{dT_{\text{PV/T}}}{d\tau} + Q_{\text{amb}} + Q_{\text{sky}} \tag{1}$$

$$Q_{\text{air}} = K_{\text{g-amb}} (T_{\text{g}} - T_{\text{amb}}) \tag{2}$$

$$Q_{\text{sky}} = \varepsilon_{\text{g}} \sigma \left(T_{\text{g}}^4 - T_{\text{sky}}^4 \right) \tag{3}$$

There is an energy conservation equation for the glass cover plate [28]:

$$\rho_{\text{g}} c_{\text{g}} \delta_{\text{g}} \frac{dT_{\text{g}}}{d\tau} = \alpha_{\text{g}} I + K_{\text{EVA-g}} (T_{\text{EVA,u}} - T_{\text{g}}) - Q_{\text{air}} - Q_{\text{sky}} \tag{4}$$

For the upper EVA adhesive, the energy conservation equation is as follows [28]:

$$\rho_{\text{EVA}} c_{\text{EVA}} \delta_{\text{EVA,u}} \frac{dT_{\text{EVA,u}}}{d\tau} = K_{\text{PV-EVA,u}} (T_{\text{PV}} - T_{\text{EVA,u}}) - K_{\text{g-EVA,u}} (T_{\text{EVA,u}} - T_{\text{g}}) \tag{5}$$

For the photovoltaic panel, the energy conservation equation is as follows [28]:

$$\rho_{\text{PV}} c_{\text{PV}} \delta_{\text{PV}} \frac{dT_{\text{PV}}}{d\tau} = \alpha_{\text{PV}} \beta_{\text{g}} I - K_{\text{PV-EVA,u}} (T_{\text{PV}} - T_{\text{EVA,u}}) - K_{\text{PV-EVA,d}} (T_{\text{PV}} - T_{\text{EVA,d}}) - E_{\text{PV}} \tag{6}$$

For the lower EVA adhesive, the energy conservation equation is as follows [28]:

$$\rho_{\text{EVA}} c_{\text{EVA}} \delta_{\text{EVA,d}} \frac{dT_{\text{EVA,d}}}{d\tau} = K_{\text{PV-EVA,d}} (T_{\text{PV}} - T_{\text{EVA,d}}) - K_{\text{al-EVA,d}} (T_{\text{EVA,d}} - T_{\text{al}}) \tag{7}$$

For the collector aluminum plates, there is an energy conservation equation [28]:

$$\rho_{\text{al}} c_{\text{al}} d_{\text{al}} \frac{dT_{\text{al}}}{d\tau} = K_{\text{al-EVA,d}} (T_{\text{EVA,d}} - T_{\text{al}}) - K_{\text{al-f}} (T_{\text{al}} - T_{\text{f}}) \tag{8}$$

For the cooling medium inside the collector, there is an energy conservation equation [28]:

$$\frac{1}{2} m_{\text{f}} c_{\text{p,f}} \left(\frac{dT_{\text{f,in}}}{d\tau} + \frac{dT_{\text{f,out}}}{d\tau} \right) = A_{\text{al}} K_{\text{al-w}} \Delta T_{\text{f}} - \dot{m}_{\text{f}} c_{\text{p,f}} (T_{\text{f,out}} - T_{\text{f,in}}) \tag{9}$$

2.2. Optoelectronic Effect Model

For the establishment of the photovoltaic power generation models, the empirical formula method is often used in engineering applications, and the key factor is the temperature of the photovoltaic cell. The empirical formulae for the efficiency of photovoltaic power generation and the temperature of the photovoltaic cells are as follows [29]:

$$\eta_{PV} = \eta_{s,PV}\left[1 - K_p(T_{PV} - T_{s,PV})\right] \tag{10}$$

$$E_{pv} = \eta_{pv}\alpha_{pv}\beta_g I \tag{11}$$

The meanings and units of symbols in the above formulas are shown in Table 1.

Table 1. Symbols.

Symbols	Meaning	Unit
Q_{solar}	The solar radiation energy absorbed by the PV/T photovoltaic thermal module per unit area	$W{\cdot}m^{-2}$
E_{PV}	The power generation of photovoltaic cells per unit area	$W{\cdot}m^{-2}$
Q_f	The heat absorbed by the cooling working fluid per unit heat exchange area in the collector	$W{\cdot}m^{-2}$;
$\rho_{PV/T}$	The average density of a collector [10]	$kg{\cdot}m^{-3}$
$c_{PV/T}$	The specific heat capacity of the collector	$J{\cdot}kg^{-1}{\cdot}K^{-1}$
$\delta_{PV/T}$	The thickness of the PV/T module	m
Q_{amb}	The convective heat transfer of air per unit area of glass cover plate	$W{\cdot}m^{-2}$
Q_{sky}	The radiant heat transfer per unit area of glass cover plate to the sky	$W{\cdot}m^{-2}$
$K_{g\text{-}amb}$	The heat transfer coefficient between glass and air	$W{\cdot}m^{-2}{\cdot}K^{-1}$
T_g	The glass cover plate temperature	K
T_{amb}	The ambient temperature	K
ε_g	The emissivity of the glass cover plate	-
σ	The Stefan Boltzmann constant, 5.67×10^{-8}	$W{\cdot}m^{-2}{\cdot}K^{-4}$
T_{sky}	The sky background temperature	K
α_g	The absorption rate of solar radiation by the glass cover plate	-
I	The solar radiation intensity projected onto the surface of the PV/T photovoltaic thermal module	$W{\cdot}m^{-2}$;
$K_{EVA\text{-}g}$	The heat transfer coefficient between the upper EVA adhesive and the glass cover plate	$W{\cdot}m^{-2}{\cdot}K^{-1}$
$T_{EVA,u}$	The temperature of the upper EVA adhesive	K
$K_{PV\text{-}EVA,u}$	The heat transfer coefficient between the photovoltaic panel and the upper EVA adhesive	$W{\cdot}m^{-2}{\cdot}K^{-1}$
T_{PV}	The temperature of the photovoltaic panel	K
β_g	The transmittance of the glass cover plate to solar radiation	-
$K_{PV\text{-}EVA,d}$	The heat transfer coefficient between the photovoltaic panel and the lower EVA adhesive	$W{\cdot}m^{-2}{\cdot}K^{-1}$
$T_{EVA,d}$	The temperature of the lower EVA adhesive	K
$K_{al\text{-}EVA,d}$	The heat transfer coefficient between the lower EVA adhesive and the collector aluminum plate	$W{\cdot}m^{-2}{\cdot}K^{-1}$
T_{al}	The temperature of the collector aluminum plate	K
$K_{al\text{-}f}$	The heat transfer coefficient between the collector aluminum plate and the cooling medium	$W{\cdot}m^{-2}{\cdot}K^{-1}$
T_f	The temperature of the cooling working fluid inside the PV/T photovoltaic thermal module	K
m_f	The mass of the cooling working fluid inside the collector	kg
$T_{f,out}$, $T_{f,in}$	The temperature of the cooling medium entering and exiting the collector	K
A_{al}	The area of the collector aluminum plate	m^2
ΔT_f	The average heat transfer temperature difference between the collector aluminum plate and the cooling working fluid of the collector	K
$\dot{m}_f$	The mass flow rate of the cooling working fluid inside the PV/T photovoltaic thermal module	$kg{\cdot}s^{-1}$
η_{PV}	The actual photovoltaic conversion efficiency of photovoltaic cells	-
$\eta_{s,PV}$	The photoelectric conversion efficiency of photovoltaic cells under a standard laboratory environment	-
K_p	The temperature coefficient for monocrystalline silicon and polycrystalline silicon photovoltaic cells, with its value generally taken as 0.0045	K^{-1}
$T_{s,PV}$	The testing temperature under standard conditions for photovoltaic cells, generally 25 °C, which is 298.15 K	K
α_{PV}	The rate of solar radiation absorption by the glass cover plate of the PV/T module	-

3. Dynamic Simulation Model of PV/T Modules and Heat Pump System

3.1. Models of PV/T Modules and Heat Pump System

A dynamic simulation model of the PV/T photovoltaic thermal modules is shown in Figure 3. At the beginning of the simulation, the instantaneous power generation and photovoltaic efficiency per unit area are calculated based on the initial temperature of the inlet cooling water of the PV/T photovoltaic thermal modules set in the evaporator, the outlet water temperature of the cooling water set in the PV/T modules, the initial temperature of the glass cover plate, and the PV plate and PV/T aluminum plate in the first time step. The PV/T modules call the solar radiation intensity function, ambient temperature function, daily average wind speed, and initial temperature values of various components of the PV/T modules. By solving the energy equation of each part of the PV/T modules, the outlet temperature of the cooling water and the temperature of each component of the PV/T modules in the second time step are obtained.

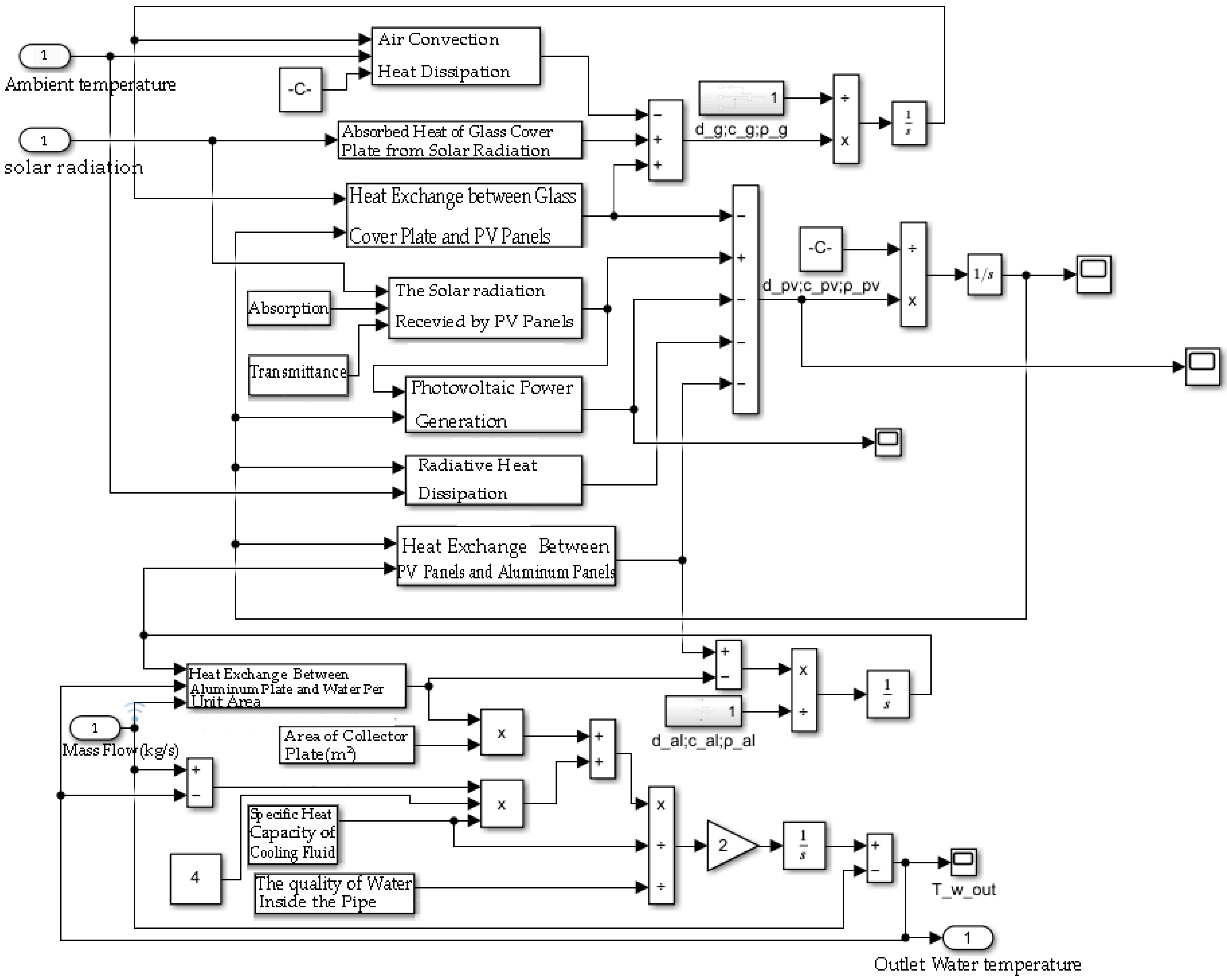

Figure 3. PV/T photothermal module model of heat pump system.

The dynamic simulation model of the whole system is shown in Figure 4. The simulated variable of the system is time, measured in seconds. At the beginning of the simulation, the system calls the initial values of each module set and calculates the corresponding working fluid parameters based on these initial values and the data entering different modules of the system for subsequent simulation calculations. Considering the long simulation time and the continuous and slow-changing trend of the parameters involved, a variable step solver is used to improve the solving efficiency. The solving method adopts ode15 s for the simulation calculation.

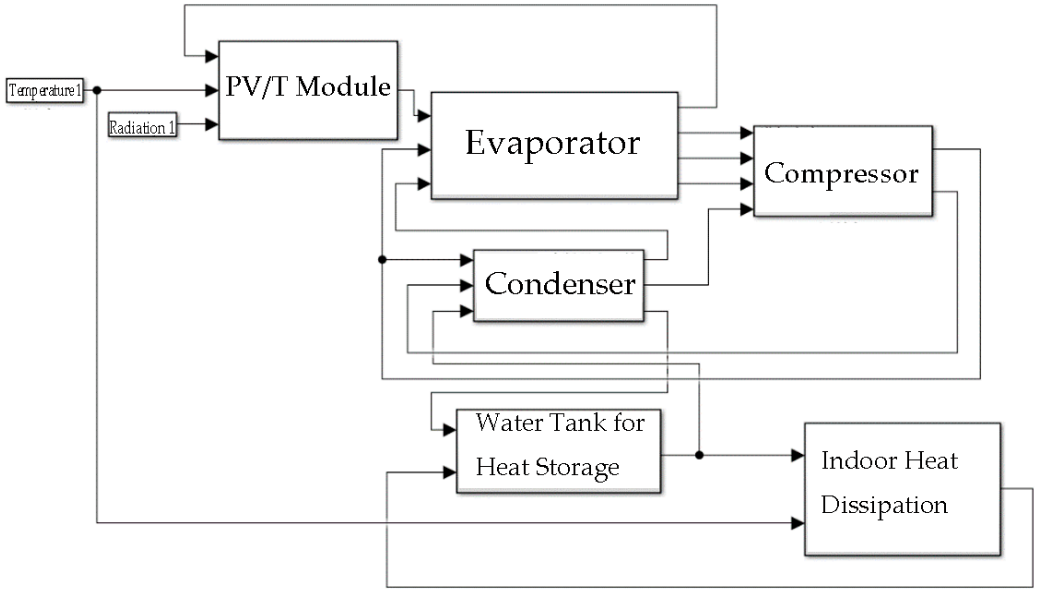

Figure 4. PV/T heat pump system model.

3.2. Model Verification

Based on the PV/T photovoltaic thermal module model and the dynamic simulation model of the entire heat pump system established in the previous part, a simulation was conducted on the photovoltaic and photothermal integration demonstration project for the Building 24 Power Station of the China Institute of Metrology. According to the results, the operating characteristics of the PV/T modules were predicted and analyzed under different summer and winter conditions. In order to meet the required solar radiation intensity for operation of the heat pump system, the simulation time was set at 8:00–18:00 in summer and 9:00–17:00 in winter.

The model was verified using the SISi thin-film-building photovoltaic photothermal integrated system, which mainly includes SI photovoltaic modules; heat pump systems; and measurement and data acquisition systems, among which the SI photovoltaic modules are composed of SI photovoltaic modules, photovoltaic inverters, and AC combiner boxes. The system uses eight SI thin-film modules, the volume of the hot water storage tank is 150 L, and the test sampling time interval is 10 min. The test time was selected on 21 December; the location was located in Baiyin City, Gansu Province; the solar radiation function for simulation calculation was fitted according to the measured meteorological parameters; and the fitting function and the measured values are shown in Figure 5. Due to frequent temperature fluctuations and the small range of numerical fluctuations, the average temperature was used for the simulation calculations. The operating characteristics of the PV/T heat pump system when used for hot water production were tested, and the test results were compared with the simulation.

Figure 6 shows the evaporation temperature and condensation temperature of the PV/T heat pump in the test system after 9:30 as a function of the test time.

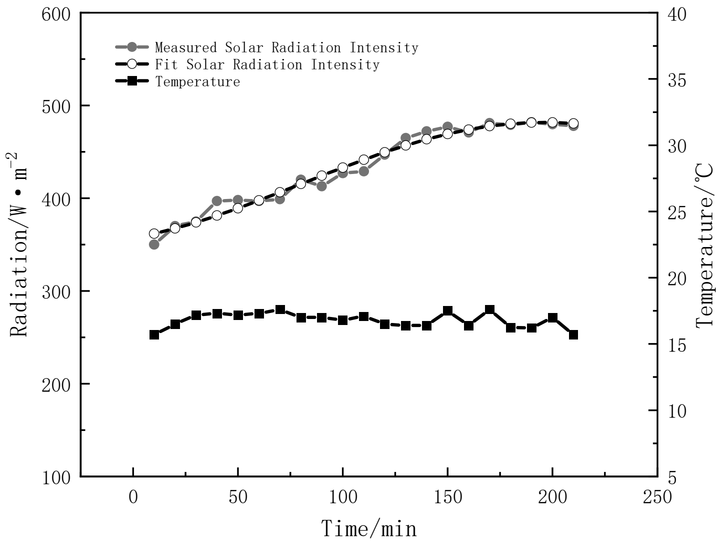

Figure 5. Meteorological parameters and fitting solar radiation intensity maps.

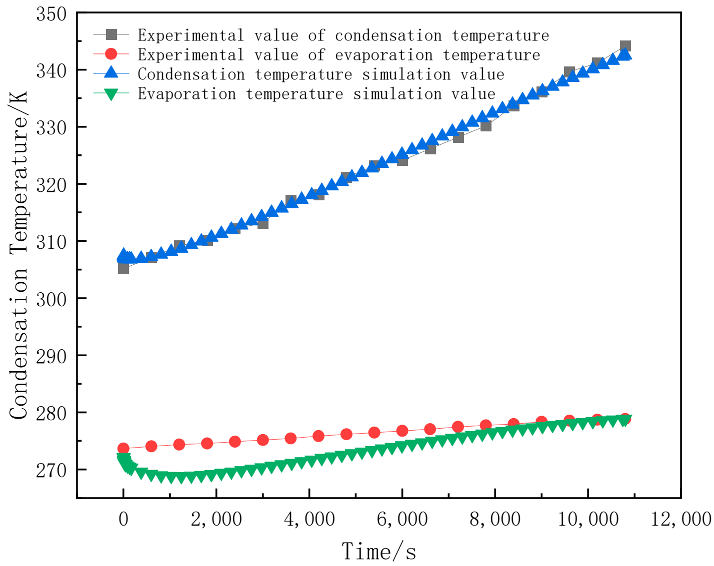

Figure 6. Evaporation and condensation temperatures over time.

As can be seen from the figure, at the beginning of the test, with the increase in solar radiation intensity, the temperature of the PV/T collector increased, the evaporation temperature rose, and the temperature rose from 0.5 °C to 5 °C because the heat pump system was used for hot water; as the test progressed, the water temperature in the hot water storage tank gradually increased, resulting in the condensation temperature also rising from 32 °C to 71 °C. The simulated condensation temperature was basically consistent with the test results, and the temperature decrease in the simulated evaporation temperature in the early stage of simulation was due to the fact that the model only considered the transfer of refrigerant energy in the system in the calculation and did not consider its temperature transfer. So, the refrigerant temperature in the evaporator decreased at the beginning of the test and then began to increase with the solar radiation intensity, which is similar to the test value in the later stage of the simulation, and this trend was basically consistent. Figure 7 shows the water temperature change curve of the water in the hot water storage tank during the heating from room temperature to 45 °C (318 K). It can be seen from the figure that the simulation results show that the water temperature rose from 12 °C to 45.3 °C in 10,800 s, that is, 180 min; the initial water temperature of the test was about 13 °C; and the temperature rose to 45 °C after 180 min.

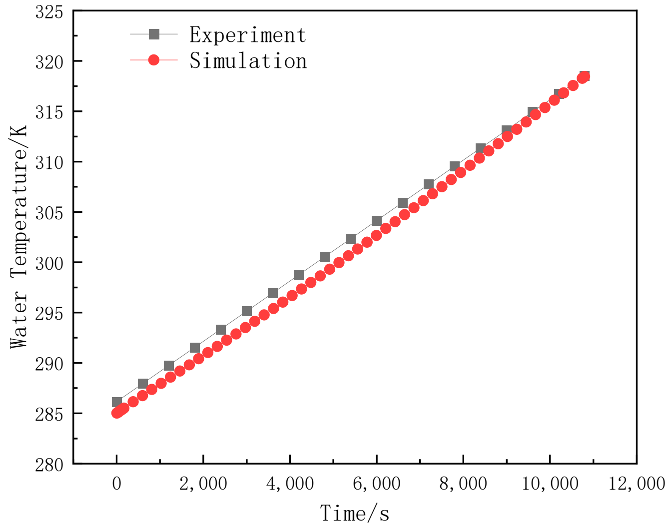

Figure 7. Water temperature curve.

Figure 8 shows the power curve of the compressor during the heat pump system test. It can be seen from the figure that the compressor power of the test system gradually increased as the test progressed, from about 33 W at the beginning to about 610 W at the end of the test, with an average power of 489 W. And, the compressor power calculated by simulation also increased with time, the compressor power at the beginning of the simulation was 287 W, that at the end was 601 W, and the average power was 401 W. The main reason for the difference is that the compressor model used in the simulation calculation adopts the empirical formula, and the calculation of its power is greatly affected by the inlet parameters of the evaporator. The temperature of the evaporator was lower than the experimental temperature during the simulation period; the overall temperature was low, so the compressor inlet parameters were low; and the calculated compressor power was smaller than that of the test.

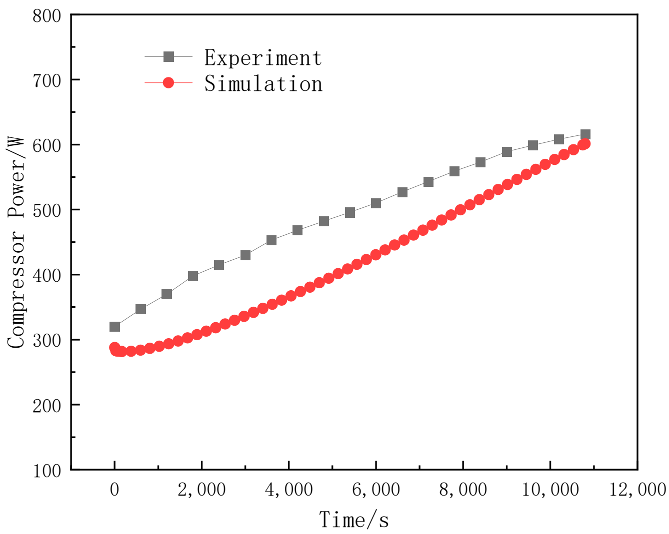

Figure 8. Compressor power change curve.

In conclusion, the model has good reliability in reflecting the working characteristics of a PV/T heat pump system during a heating operation, which can be used to predict the operating characteristics of a heat pump system.

4. Analysis of Simulation Results

Based on the PV/T photovoltaic thermal module model and the dynamic simulation model of the entire heat pump system established in the previous part, simulation research was conducted on the photovoltaic and photothermal integration demonstration project for the Building 24 Power Station of the China Institute of Metrology. According to the results, the operating characteristics of the PV/T modules were predicted and analyzed under different summer and winter heating conditions. In order to meet the required solar radiation intensity for operation of the heat pump system, the simulation time was set at 8:00–18:00 in summer and 9:00–17:00 in winter. The medium in the PV/T modules was water. The initial conditions are shown as Table 2.

Table 2. Initial conditions.

Basic Parameters	Value
Absorptivity	0.9
Transmittance	0.9
The initial temperature of the cooling fluid (°C)	6.85
Wind velocity (m/s)	2.68
Specific heat capacity of cooling medium	3000
The quality of the water in the pipe (kg)	1000
Hot plate area (m^2)	432

4.1. Simulation Analysis under Summer Heating Conditions

The simulation started from 8:00 and ends at 18:00 Beijing time. The solar radiation intensity increased with system operating time, reached its maximum at 13:00, and then continued to decrease until the end of the simulation. The meteorological parameters were fit and imported into the simulation model for calculation [30].

A temperature comparison between the PV/T photovoltaic thermal modules and ordinary photovoltaic cell modules is shown in Figure 9a. It can be seen that the temperature change trends of the two modules are similar, both increasing and decreasing with the change in solar irradiance. But, there are significant differences in the temperature changes between the two modules. From the beginning of the simulation, the temperature of the ordinary photovoltaic module panel increased from 22.5 °C and continued to increase to the maximum, at 63.4 °C, after about 5.5 h with the increase in solar radiation intensity; then decreased with the weakening of solar radiation intensity; and finally reduced to 36.2 °C at the end of the simulation. The average temperature of the ordinary photovoltaic modules throughout the entire operation cycle was 35.4 °C. While the temperature of PV/T modules first decreased at the initial simulation stage, it rapidly dropped from the initial 22.5 °C to around 2.8 °C after about 0.6 h. Then, with the solar radiation intensity increases, the temperature of the PV/T modules increased to around 21.9 °C after about 5.5 h and then began to decrease again. The average temperature throughout the entire circulation operation was only about 15.2 °C, which is 20.2 °C lower than the average temperature of the ordinary photovoltaic panel.

The reason for the temperature decreasing for the PV/T modules during the initial stage is the circulating effect of the internal medium, which can cool the PV/T modules and take away the generated heat quickly. Furthermore, at the initial stage, the solar radiation intensity was low and the temperature of the whole heat pump system was also low. As the solar radiation intensity increased, the remaining heat from photoelectric conversion increased and could not be taken away by the medium in time. Therefore, the surface temperature of the components gradually increased, reached its maximum value after 5.5 h, and then decreased with the weakening of solar radiation intensity afterwards. During the entire operation period, the temperature of the PV/T modules was lower than that of the ordinary photovoltaic panel for the cooling medium inside and the panel continuously circulated and transferred the remaining heat from the photovoltaic conversion to the evaporator of the heat pump system. Finally, the heat was transferred by the refrigerant to the condenser for release, achieving a continuous cooling effect for the PV/T modules, meanwhile providing heat for thermal users.

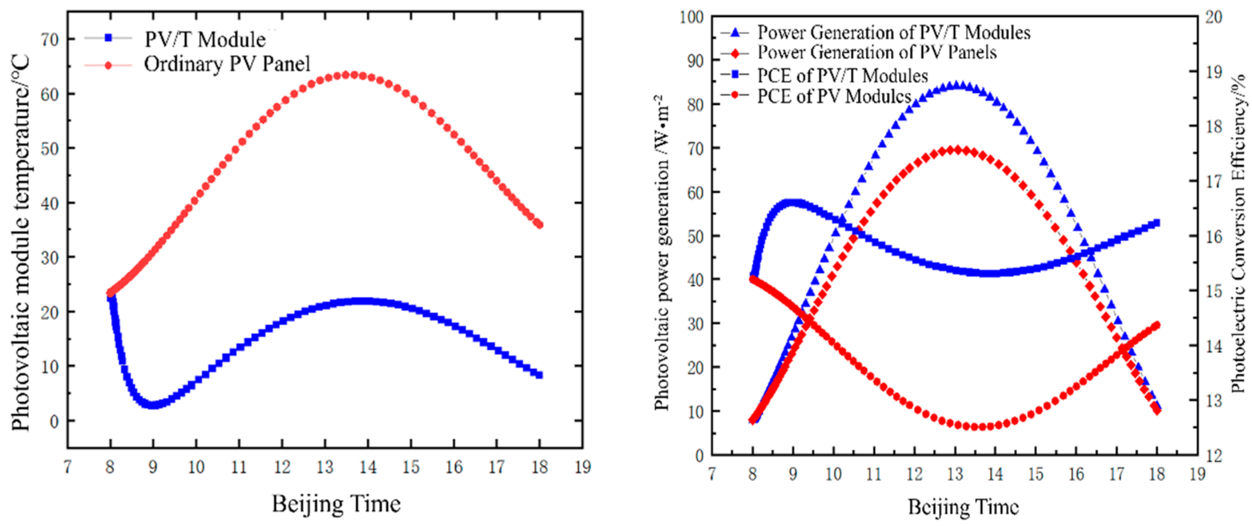

(**a**) (**b**)

Figure 9. (**a**) Temperature comparison between PV/T modules and ordinary photovoltaic panel (summer conditions); (**b**) comparison of photovoltaic conversion characteristics between PV/T modules and ordinary panel (summer conditions).

The operating results also indicate that the difference between the highest and lowest operating temperatures of the PV/T modules is 19.1 °C, while the temperature difference in the ordinary photovoltaic panel is 40.9 °C. This is because the circulating working fluid in the PV/T modules has a certain heat capacity, which reduces the temperature change amplitude and weakens the temperature fluctuation. Therefore, the conversion efficiency of photovoltaic power generation further increases, and the photovoltaic power generation is significantly improved simultaneously.

A comparison of the photovoltaic conversion characteristics between the PV/T modules and the ordinary photovoltaic panel is shown in Figure 9b. The results show that there is not much difference in power generation and photovoltaic efficiency between the two modules at the beginning of the simulation. As the solar radiation intensity increases, the photovoltaic power generation of the two modules both increases. At around 1:00 pm, when the solar radiation intensity reached its maximum value, the photovoltaic power generation of the two modules both reached their maximum values. But, the maximum values were different. The power generation of the ordinary panel was 69 W·m^{-2}, while the power generation of the PV/T module was 84 W·m^{-2}, which is about 21% higher than that of the ordinary panel. During the simulation period, the photovoltaic efficiency of the ordinary panel was 13.6%, and the average photovoltaic efficiency of the PV/T module was 15.7% which is 15.4% higher. This is because in the early stages of operation, the solar radiation intensity is relatively low, and the temperatures of the PV/T module and the ordinary panel are similar. So, the photovoltaic efficiency is similar. Subsequently, due to the operation of the heat pump system, the cooling medium inside the PV/T module continuously carries away the waste heat generated by the photovoltaic conversion, making its temperature rise more slowly, and the photovoltaic conversion efficiency is thus significantly improved compared to that of the ordinary panel, resulting in an increase in power generation.

4.2. Simulation Analysis under Winter Heating Conditions

The simulation started from 9:00 and ended at 17:00 Beijing time, and the changes in meteorological parameters were similar to those in summer. The solar radiation intensity first increased, then reached its maximum value at 13:00, and finally continuously decreased until the simulation ended.

A temperature comparison between the PV/T module and the ordinary photovoltaic panel under winter heating conditions is shown in Figure 10a. At the beginning of the simulation, the temperature of the ordinary panel gradually increased with the increase in solar radiation intensity. After 4.2 h, it rose from the initial 5.0 °C to 27.9 °C and then began to decrease. At the end of the simulation, it dropped to 10.1 °C. The average surface temperature of the panel was 18.3 °C. While the temperature of the PV/T modules rapidly decreased from 5.0 °C at the beginning of operation to −8.6 °C for the initial 0.6 h, it then increased with the increase in solar radiation intensity. Influenced by the operation of the heat pump system, after about 4.5 h, the temperature of the PV/T module just increased to 4.4 °C and then gradually decreased. During the simulation period, the average temperature of the collector was 0.5 °C, which was 17.8 °C lower than that of the ordinary panel.

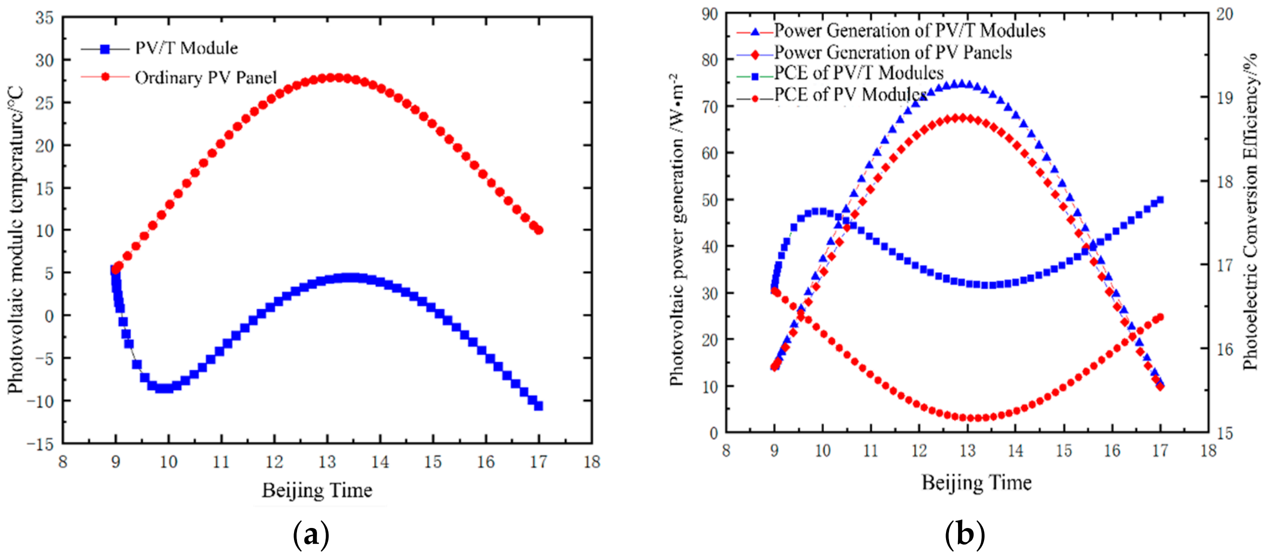

Figure 10. (**a**) Temperature comparison between the PV/T modules and an ordinary PV panel (winter conditions); (**b**) comparison of the photovoltaic conversion characteristics between the PV/T module and an ordinary PV panel (winter conditions).

A comparison of the photovoltaic conversion characteristics between the PV/T module and the ordinary photovoltaic panel is shown in Figure 10b. The photovoltaic conversion characteristics of both modules were similar to those of the summer operating conditions. The power generation and photovoltaic conversion efficiency of the PV/T modules were higher than those of an ordinary panel. The maximum power generation of the PV/T modules was 74.6 $W \cdot m^{-2}$, which was 10.5% higher than the 67.5 $W \cdot m^{-2}$ of the ordinary panel. The average photovoltaic conversion efficiency of the PV/T modules was 17.2%, which increased by 8.9% compared with the 15.8% of the ordinary panel. However, due to the weakening of solar radiation intensity in winter compared with the summer conditions, the ambient temperature was lower and the surface temperatures of the PV/T module and the ordinary panel both decreased. Therefore, the photoelectric conversion efficiencies of both modules improved compared with the summer conditions, both reaching over 15%. The photovoltaic conversion efficiency of the PV/T module significantly improved compared to that of the ordinary photovoltaic panel, but the improvement effect was smaller than that of the summer conditions.

5. Conclusions

In this article, dynamic models of components contained in a PV/T heat pump system were established using energy conservation formulas. Also, the simulation was conducted based on the Simulink software for the PV/T modules and the whole system applied in the photovoltaic photothermal integration demonstration project for Building 24 Power Station of the China Institute of Metrology. The working characteristics of the system were simulated under two typical summer and winter working conditions. The results show that under summer conditions, the average temperature of the PV/T modules is 20.2 °C lower than that of an ordinary photovoltaic panel and the average photoelectric conversion efficiency increases by 15.4%. Under the winter operating conditions, the average temperature of the PV/T module is 17.8 °C lower than that of photovoltaic panel, and the average photoelectric efficiency is 8.9% higher. The results show that under different operating conditions, the surface temperature of the PV/T modules is significantly lower than that of an ordinary panel, and the photoelectric conversion efficiency and power generation are both significantly improved.

Author Contributions: Conceptualization, T.S., Z.L. and Y.G.; writing—original draft preparation, G.G.; writing—review and editing, Y.A. and Y.F.; supervision, Q.L. and X.Z. All authors have read and agreed to the published version of the manuscript.

Funding: A project funded by the China Institute of Metrology (CMI) with its own funds, ZYZJ2302.

Data Availability Statement: Data is contained within the article.

Conflicts of Interest: The authors declare no conflicts of interest.

References

1. Dubey, S.; Sarvaiya, J.N.; Seshadri, B. Temperature dependent photovoltaic (PV) efficiency and its effect on PV production in the world—A review. *Energy Procedia* **2013**, *33*, 311–321. [CrossRef]
2. Wolf, M. Performance analyses of combined heating and photovoltaic power systems for residences. *Energy Convers.* **1976**, *16*, 79–90. [CrossRef]
3. Kern, J.E.C.; Russell, M.C. Combined Photovoltaic and Thermal Hybrid Collector Systems. In Proceedings of the IEEE Photovoltaic Specialists, Washington, DC, USA, 5 June 1978.
4. Ito, S.; Miura, N.; Takano, Y. Studies of heat pumps using direct expansion type solar collectors. *J. Sol. Energy Eng.* **2005**, *127*, 60–64. [CrossRef]
5. Pei, G.; Jie, J.; Wei, H.; Liu, K. Performance of photovoltaic solar assisted heat pump system in typical climate zone. *J. Energy Environ.* **2007**, *6*, 1–9.
6. Ji, J.; Pei, G.; Chow, T.T.; Liu, K.; He, H.; Lu, J.; Han, C. Experimental study of photovoltaic solar assisted heat pump system. *Sol. Energy* **2008**, *82*, 43–52. [CrossRef]
7. Zhang, X.; Zhao, X.; Smith, S.; Xu, J.; Yu, X. Review of R&D progress and practical application of the solar photovoltaic/thermal (PV/T) technologies. *Renew. Sustain. Energy Rev.* **2012**, *16*, 599–617.
8. Solanki, S.C.; Dubey, S.; Tiwari, A. Indoor simulation and testing of photovoltaic thermal (PV/T) air collectors. *Appl. Energy* **2009**, *86*, 2421–2428. [CrossRef]
9. Shyam, A.; Tiwari, G.N.; Al-Helal, I.M. Analytical expression of temperature dependent electrical efficiency of N-PVT water collectors connected in series. *Sol. Energy* **2015**, *114*, 61–76. [CrossRef]
10. Jouhara, H.; Milko, J.; Danielewicz, J.; Sayegh, M.A.; Szulgowska-Zgrzywa, M.; Ramos, J.B.; Lester, S.P. The performance of a novel flat heat pipe based thermal and PV/T (photovoltaic and thermal systems) solar collector that can be used as an energy-active building envelope material. *Energy* **2016**, *108*, 148–154. [CrossRef]
11. Li, H.; Sun, Y.; Fu, X.S. A novel solar photovoltaic loop heat pipe/heat pump water heating system. *Acta Energ. Sol. Sin.* **2020**, *41*, 59–66.
12. Chen, H.B.; Zhang, X.K.; Wang, C.C.; Li, S.Q.; Yao, H.N.; Gong, Y.T. An experimental research on energy-saving efficiency of a solar PV/T heat pump system based on micro heat pipe array. *Renew. Energy Resour.* **2021**, *39*, 611–617.
13. Chu, L.C.; Zhao, S.G.; Gao, Y.Z.; Liu, C.; Zhang, X.S. Experimental study on performance of photovoltaic direct-driven PV/T dual-source heat pump hot water system. *Acta Energ. Sol. Sin.* **2023**, *44*, 188–194.
14. Fu, L.; Ding, G.L.; Zhang, C.L. Dynamic Simulation of Air-to-Water Dual-Mode Heat Pumps. *J. Eng. Thermophys.* **2003**, *24*, 725–728.
15. Mastrullo, R.; Renno, C.A. Thermoeconomic model of a photovoltaic heat pump. *Appl. Therm. Eng.* **2010**, *30*, 1959–1966. [CrossRef]

16. Khelifa, A.; Touafek, K.; Moussa, H.B.; Tabet, I. Modeling and detailed study of hybrid photovoltaic thermal (PV/T) solar collector. *Sol. Energy* **2016**, *135*, 169–176. [CrossRef]
17. Zhang, H.; Liu, H.; Chen, H.; Guo, X.; Liang, K.; Yao, P. Research on the Performance of Flat-Box Photovoltaic/ Thermal Collector with Cooling Channels. *J. Sol. Energy Eng.* **2017**, *140*, 021002.
18. Zhou, J.; Ke, H.; Deng, X. Experimental and CFD investigation on temperature distribution of a serpentine tube type photovoltaic/thermal collector. *Sol. Energy* **2018**, *174*, 735–742. [CrossRef]
19. Dannemand, M.; Sifnaios, I.; Tian, Z.; Furbo, S. Simulation and optimization of a hybrid unglazed solar photovoltaic-thermal collector and heat pump system with two storage tanks. *Energy Convers. Manag.* **2020**, *206*, 112429. [CrossRef]
20. Kavian, S.; Aghanajafi, C.; Mosleh, H.J.; Nazari, A.; Nazari, A. Exergy, economic and environmental evaluation of an optimized hybrid photovoltaic-geothermal heat pump system. *Appl. Energy* **2020**, *276*, 115469. [CrossRef]
21. Yerdesh, Y.; Abdulina, Z.; Aliuly, A.; Belyayev, Y.; Mohanraj, M.; Kaltayev, A. Numerical simulation on solar collector and cascade heat pump combi water heating systems in Kazakhstan climates. *Renew. Energy* **2020**, *145*, 1222–1234. [CrossRef]
22. El-Hamid, M.A.; Wei, G.; Sherin, M.; Cui, L.; Du, X. Comparative study of different photovoltaic/thermal hybrid configurations from energetic and exergetic points of view: A numerical analysis. *J. Sol. Energy Eng.* **2021**, *143*, 061006. [CrossRef]
23. Heinz, A.; Rieberer, R. Energetic and economic analysis of a PV-assisted air-to-water heat pump system for renovated residential buildings with high-temperature heat emission system. *Appl. Energy* **2021**, *293*, 116953. [CrossRef]
24. Ma, X.F. Study on Dynamic Simulation and Optimization of PV/T-Heat Pump System. Master's Thesis, Qingdao University of Technological, Qingdao, China, 2018.
25. Guo, G.Z.; Gou, Y.J. Simulation and Experimental Research on Integrated System of Photovoltaic and Photothermal Based on High-Efficiency Collector. Master's Thesis, North China University of Science and Technology, Tangshan, China, 2021.
26. Wang, X.; Hao, X.J. Dynamic simulation of heating effect of different heat sources based on Simulink. *Gas Heat* **2023**, *43*, 35–42.
27. Ji, M.D.; Gou, Y.J.; Zhong, X.H. Performance simulation and analysis of photovoltaic photothermal integrated system in Baiyin area. *Integr. Intell. Energy* **2023**, *45*, 43–52.
28. Tao, W.X. *Heat Transfer*; Higher Education Press: Beijing, China, 2019.
29. Zhou, C. Investigation on the Heating, Power and Cooling Tri-Generation Performance for the Household Roll-Bond Photovoltaic Thermal Heat Pump System. Ph.D. Thesis, Dalian University of Technology, Dalian, China, 2020.
30. Da, X. *Energy Weather Platform*; North Daxian Wind Power Technology: Beijing, China, 2023; Available online: http://windgrid.dxwind.com/ (accessed on 27 March 2020).